

UNCLASSIFIED
~~RESTRICTED~~

Copy No.

6

RM No. L8E24

NACA RM No. L8E24

CLASSIFICATION CHANGED
SEP 1948

To UNCLASSIFIED

NACA

By authority of *H. L. Dryden* Date *Nov 26, 1952*

for NACA Release form #1348
By HRR, 12-24-52

RESEARCH MEMORANDUM

AERODYNAMIC CHARACTERISTICS OF A TWO-BLADE

NACA 10-(3)(08)-03R PROPELLER

By

Albert J. Evans and Leland B. Salters, Jr.

Langley Aeronautical Laboratory
Langley Field, Va.

CLASSIFIED DOCUMENT

This document contains classified information affecting the National Defense of the United States within the meaning of the Espionage Act, USC 8041 and 8042. Its transmission or the revelation of its contents in any manner to an unauthorized person is prohibited by law. Information so classified may be imparted only to persons in the military and naval services of the United States, appropriate civilian officers and employees of the Federal Government who have a legitimate interest therein, and to United States citizens of known loyalty and discretion who of necessity must be informed thereof.

NATIONAL ADVISORY COMMITTEE
FOR AERONAUTICS

WASHINGTON
September 2, 1948

~~RESTRICTED~~

UNCLASSIFIED

NACA LIBRARY
LANGLEY MEMORIAL AERONAUTICAL
LABORATORY
Langley Field, Va.

NATIONAL ADVISORY COMMITTEE FOR AERONAUTICS

RESEARCH MEMORANDUM

AERODYNAMIC CHARACTERISTICS OF A TWO-BLADE

NACA 10-(3)(08)-03R PROPELLER

By Albert J. Evans and Leland B. Salters, Jr.

SUMMARY

Full-scale tests have been made in the Langley 16-foot high-speed tunnel to determine the aerodynamic characteristics of the NACA 10-(3)(08)-03R propeller. The tests on this propeller were conducted as part of a program to determine the effects of shank design on propeller aerodynamic characteristics.

The tests were made on a 2000-horsepower dynamometer over a range of advance ratio from 0.45 to 3.6. The blade-angle range, measured at the 0.75-radius station, extended from 20° to 50° .

A maximum efficiency of 91.5 percent was attained at 1600 revolutions per minute at a blade angle of 30° . Peak efficiency at a blade angle of 45° was decreased 32 percent by an increase in helical-tip Mach number from 0.80 to 1.2.

INTRODUCTION

The NACA has recently completed the major portion of a general investigation of the mutual effects of the propeller design parameters, solidity, thickness, and camber and air compressibility. The series of propellers tested embodied systematic variations of blade-section camber, thickness, blade width, airfoil section, and shank design. The propellers, all of 10-foot diameter, were designed to have a minimum induced energy loss, or Betz loading, at the design operating condition.

This paper presents the test data obtained for the NACA 10-(3)(08)-03R propeller blade which was one of the blades tested to determine the effects of shank design. No analysis is included of the data contained herein in order to permit the earliest possible publication of the data contained in this report.

UNCLASSIFIED

~~RESTRICTED~~

APPARATUS

Propeller dynamometer.-- The tests were made on a 2000-horsepower propeller dynamometer in the Langley 16-foot high-speed tunnel. A complete description of the dynamometer is contained in reference 1.

Propeller blades.-- The propeller blades are designated the NACA 10-(3)(08)-03R design. The digits in the designation indicate a 10-foot-diameter propeller with a design lift coefficient of 0.30, a section 8 percent thick, and a solidity of 0.03 per blade at the 0.70-radius station. The R following the designation signifies a propeller blade incorporating a round shank. The blades were designed to have the Betz loading for minimum induced energy loss when operating at a blade angle of 45° at the 0.70-radius station, and as a three-blade propeller of 10-foot diameter. The Betz loading could not be achieved over the round shanks, but was carried inboard as far as possible, to approximately the 0.35-radius station. The Betz loading for a three-blade propeller operating at blade angle of 45° at the 0.70-radius station is compared with the design loading of the NACA 10-(3)(08)-03R propeller in figure 1. The Betz loading curve is taken from reference 2. The blades were tested as a two-blade propeller and blade-form characteristic curves are presented in figure 2.

Tests.-- Thrust, torque, and rotational speed were measured at each 5° increment of blade angle from 20° to 55° , inclusive, measured at the 75-percent (45-inch) radius station. A constant rotational speed was used for each test and a range of advance ratio $\left(J = \frac{V}{nD}\right)$ was covered by changing the tunnel airspeed which was varied from about 60 to 460 miles per hour. At higher blade angles the dynamometer could not deliver sufficient torque to cover the complete range of advance ratio at the higher rotational speeds and for this reason the lower rotational speeds were used for the higher blade angles.

Additional tests were made at constant high value of tunnel airspeed and variable rotational speeds in order to extend the tip Mach number range of the tests at a blade angle of 45° .

All tests were run over a range of advance ratio to determine propeller performance from maximum efficiency to zero torque.

A chart of the testing program is presented in table I.

REDUCTION OF DATA

The test results corrected for tunnel-wall interference and spinner force are presented in the form of the usual thrust and power coefficients

and propeller efficiency. A complete description of the methods used to determine the propeller coefficients is given in reference 1. The symbols and definitions used throughout this report are as follows:

b	blade chord, feet
C_{ld}	design lift coefficient
C_P	power coefficient $\left(\frac{P}{\rho n^3 D^5} \right)$
C_T	thrust coefficient $\left(\frac{T}{\rho n^2 D^4} \right)$
D	propeller diameter, feet
h	blade-section maximum thickness, feet
J	advance ratio $\left(\frac{V}{nD} \right)$
M	free-stream Mach number
M_t	helical-tip Mach number $\left(M \sqrt{1 + \left(\frac{\pi}{J} \right)^2} \right)$
n	propeller rotational speed, revolutions per second
N	propeller rotational speed, revolutions per minute
P	power absorbed by propeller, foot-pounds per second
r	radius to a blade element, feet
R	propeller-tip radius, feet
T	propeller thrust, pounds
V	free-stream velocity, feet per second
β	blade angle, degrees
η	propeller efficiency $\left(\frac{C_T J}{C_P} \right)$
ρ	mass density of air in free stream, slugs per cubic foot

RESULTS

Faired curves of thrust coefficient, power coefficient, and propeller efficiency plotted against advance ratio are presented in figures 3 to 10. Test points are shown on the figures giving thrust and power coefficient.

Shown on the propeller-efficiency curves are plots of the air-stream Mach number together with the helical-tip Mach number. The discontinuities in the Mach number curves, when plotted against advance ratio at constant rotational speed, are caused by changes in the air temperature in the tunnel between tests. The values of Mach number and helical-tip Mach number shown for the propeller data in this report are the true Mach numbers at which the data were obtained.

Envelope-efficiency curves plotted against advance ratio are presented in figure 11 for five rotational speeds. The induced efficiency of a frictionless propeller with a Betz loading operating at the same values of power coefficient as the NACA 10-(3)(08)-03R propeller at 1350 revolutions per minute is also shown on figure 11. The difference between the envelope curve for the NACA 10-(3)(08)-03R propeller at 1350 revolutions per minute and the induced-efficiency curve is the loss in efficiency due to the profile drag of the sections plus the loss due to the unfavorable loading over the inboard sections of a round-shank propeller. The induced efficiency was obtained from charts in reference 3.

Figure 12 presents the values of maximum efficiency attainable in the tests for several blade angles plotted against propeller tip Mach number.

Langley Aeronautical Laboratory
National Advisory Committee for Aeronautics
Langley Field, Va.

REFERENCES

1. Corson, Blake W., Jr., and Maynard, Julian D.: The NACA 2000-Horsepower Propeller Dynamometer and Tests at High Speed of an NACA 10-(3)(08)-03 Two-Blade Propeller. NACA RM No. L7L29, 1948.
2. Hartman, Edwin P., and Feldman, Lewis: Aerodynamic Problems in the Design of Efficient Propellers. NACA ACR, Aug. 1942.
3. Crigler, John L., and Talkin, Herbert W.: Charts for Determining Propeller Efficiency. NACA ACR No. L4I29, 1944.

TABLE I

Figure	Tunnel speed	Propeller speed (rpm)	Blade angle, β , at 0.75R (deg)							
3	Variable	1140				35	40	45	50	55
4	Variable	1350	20	25	30	35	40	45	50	
5	Variable	1600	20	25	30	35	40	45		
6	Variable	2000	20	25	30	35				
7	Variable	2160	20	25	30					
8	Variable	1500						45		
9(a)	M = 0.56	Variable						45		
9(b)	M = 0.60	Variable						45		
9(c)	M = 0.65	Variable						45		
10	M = 0.65	Variable							50	



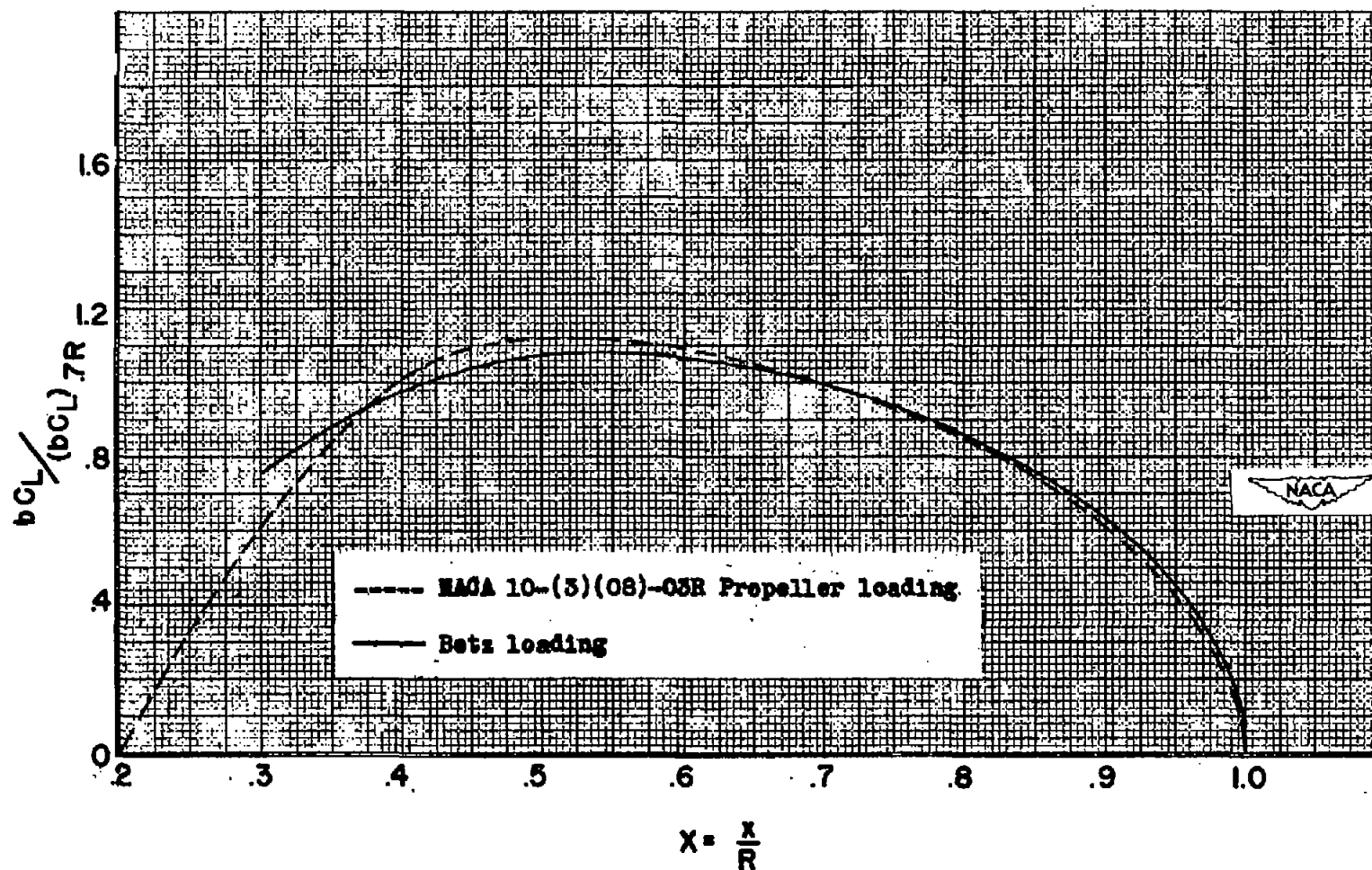


Figure 1.- Comparison of design loading of NACA 10-(3)(08)-03R propeller blade with Betz loading.

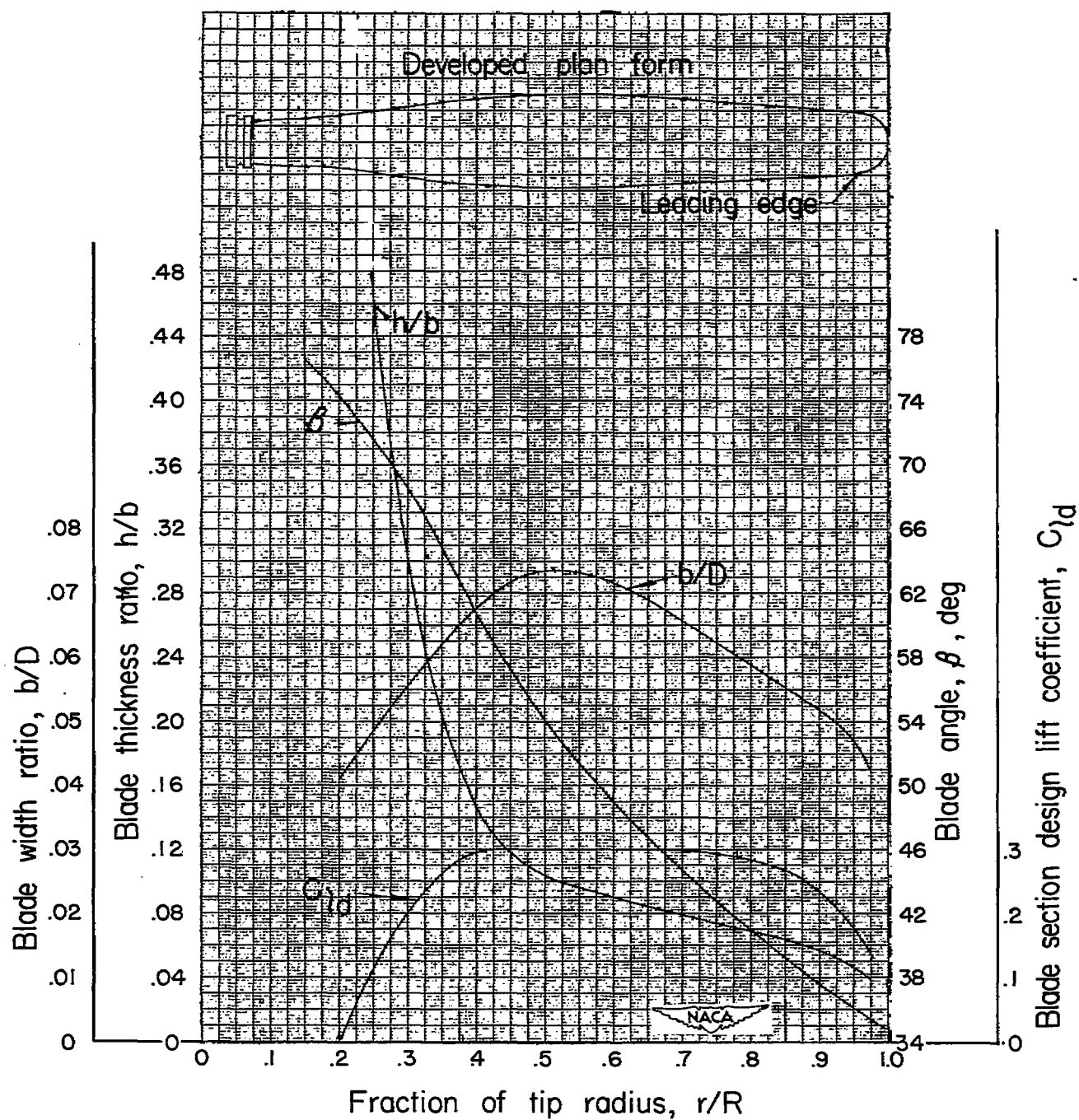
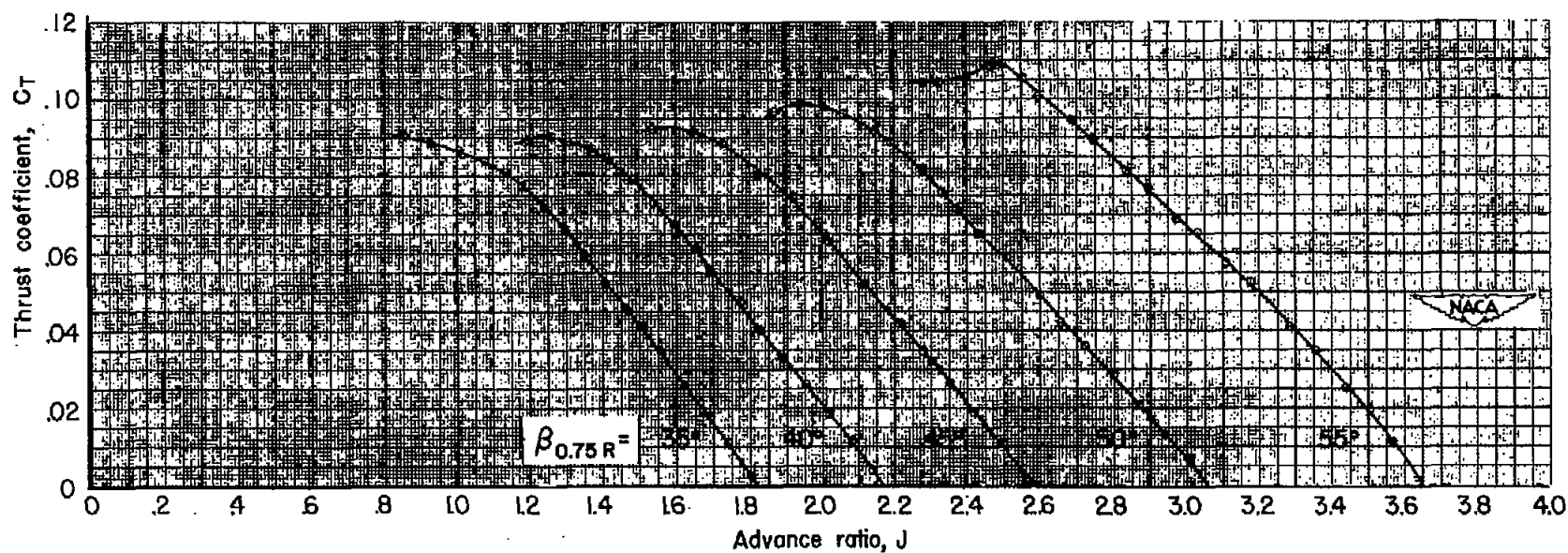
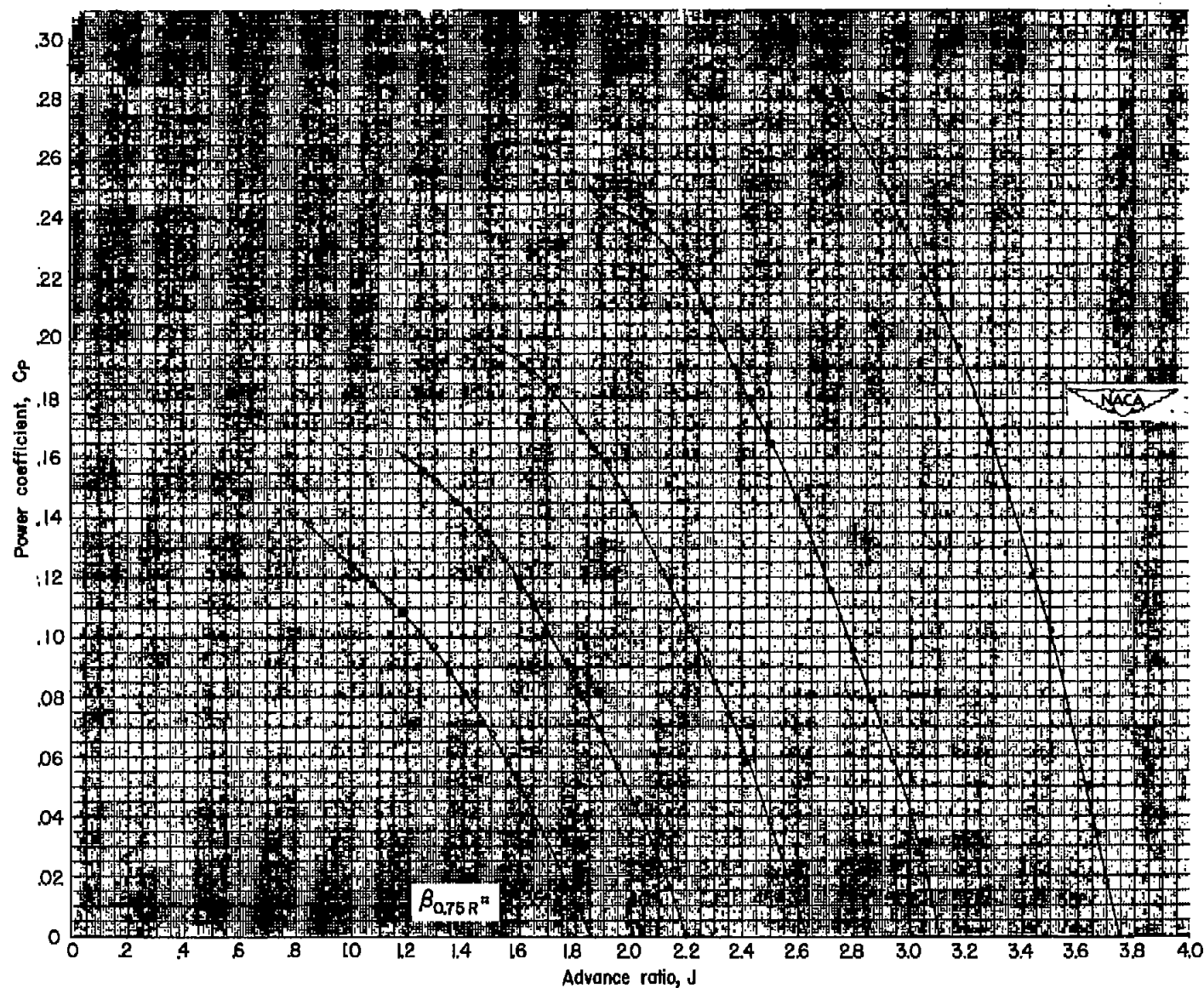


Figure 2.- Blade-form curves for NACA 10-(3)(08)-03R propeller.



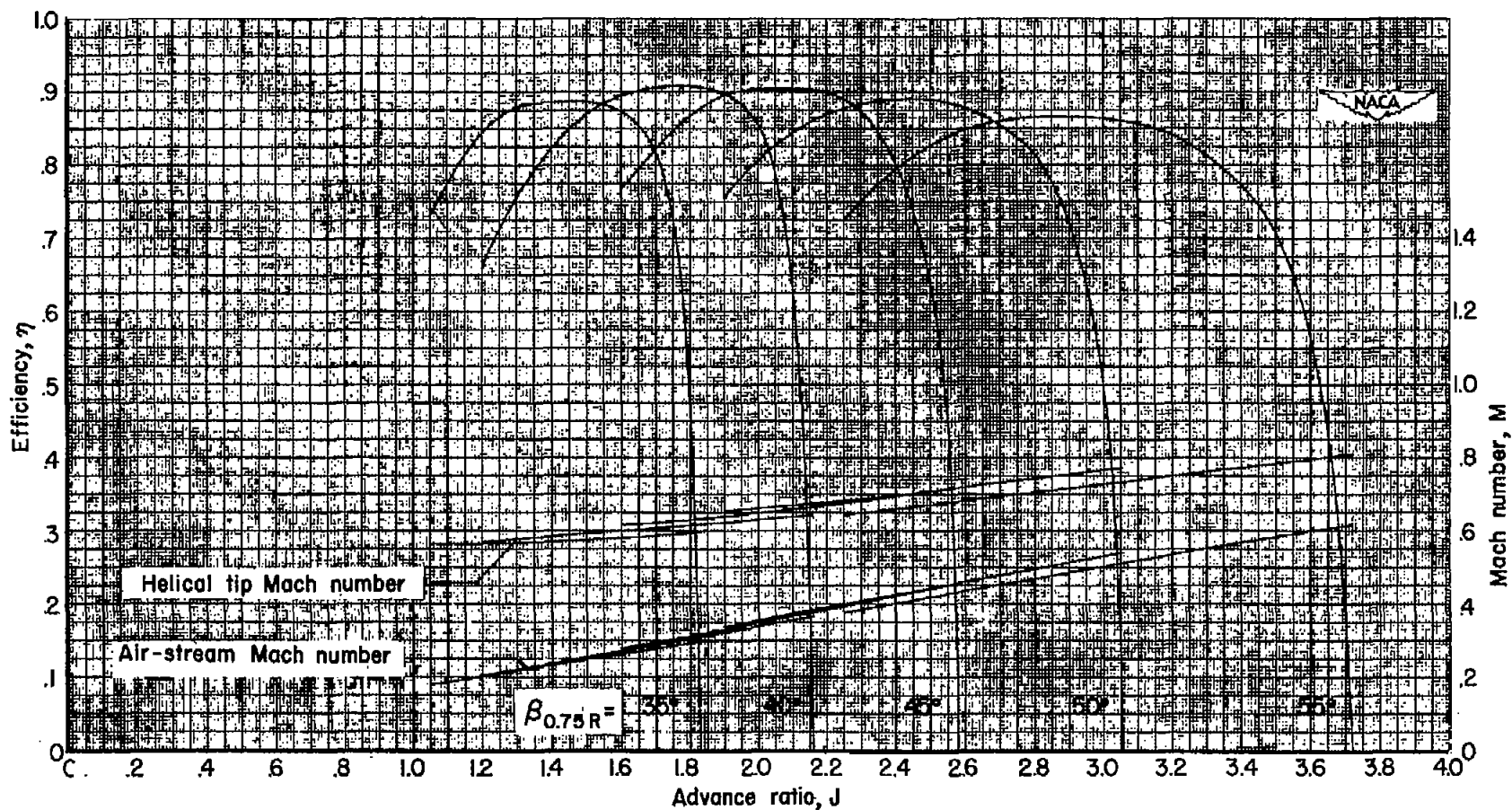
(a) Thrust coefficient.

Figure 3.- Characteristics of NACA 10-(3)(08)-03R propeller at 1140 revolutions per minute.



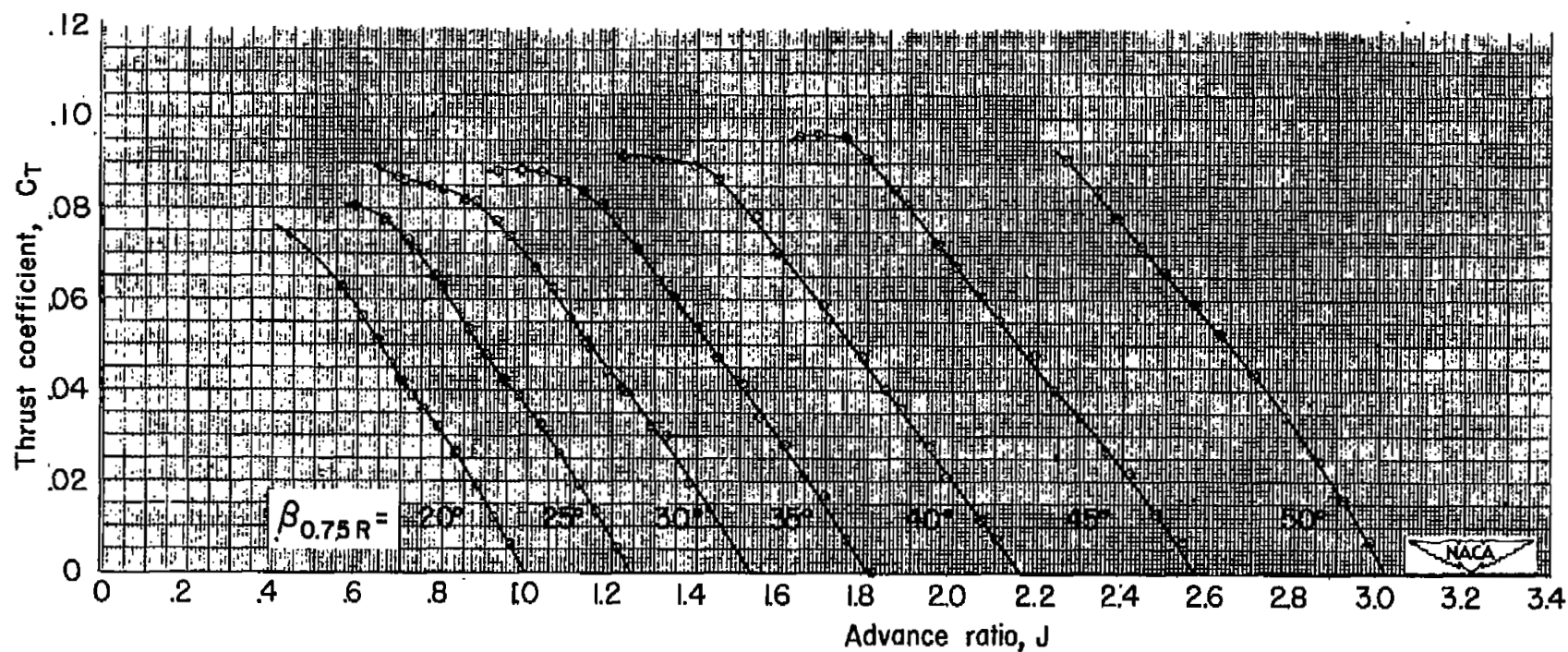
(b) Power coefficient.

Figure 3.- Continued. 1140 revolutions per minute.



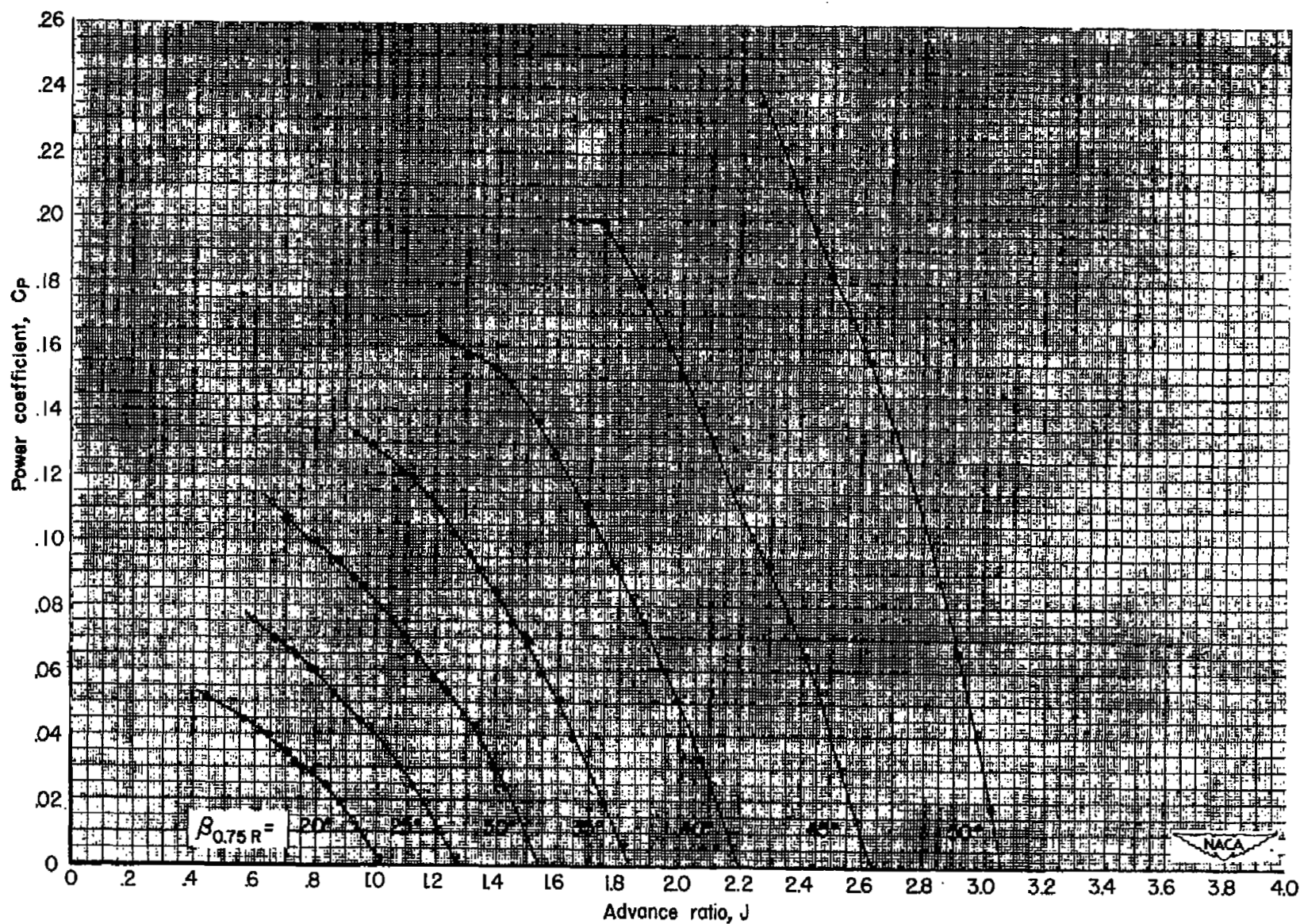
(c) Efficiency.

Figure 3.- Concluded. 1140 revolutions per minute.



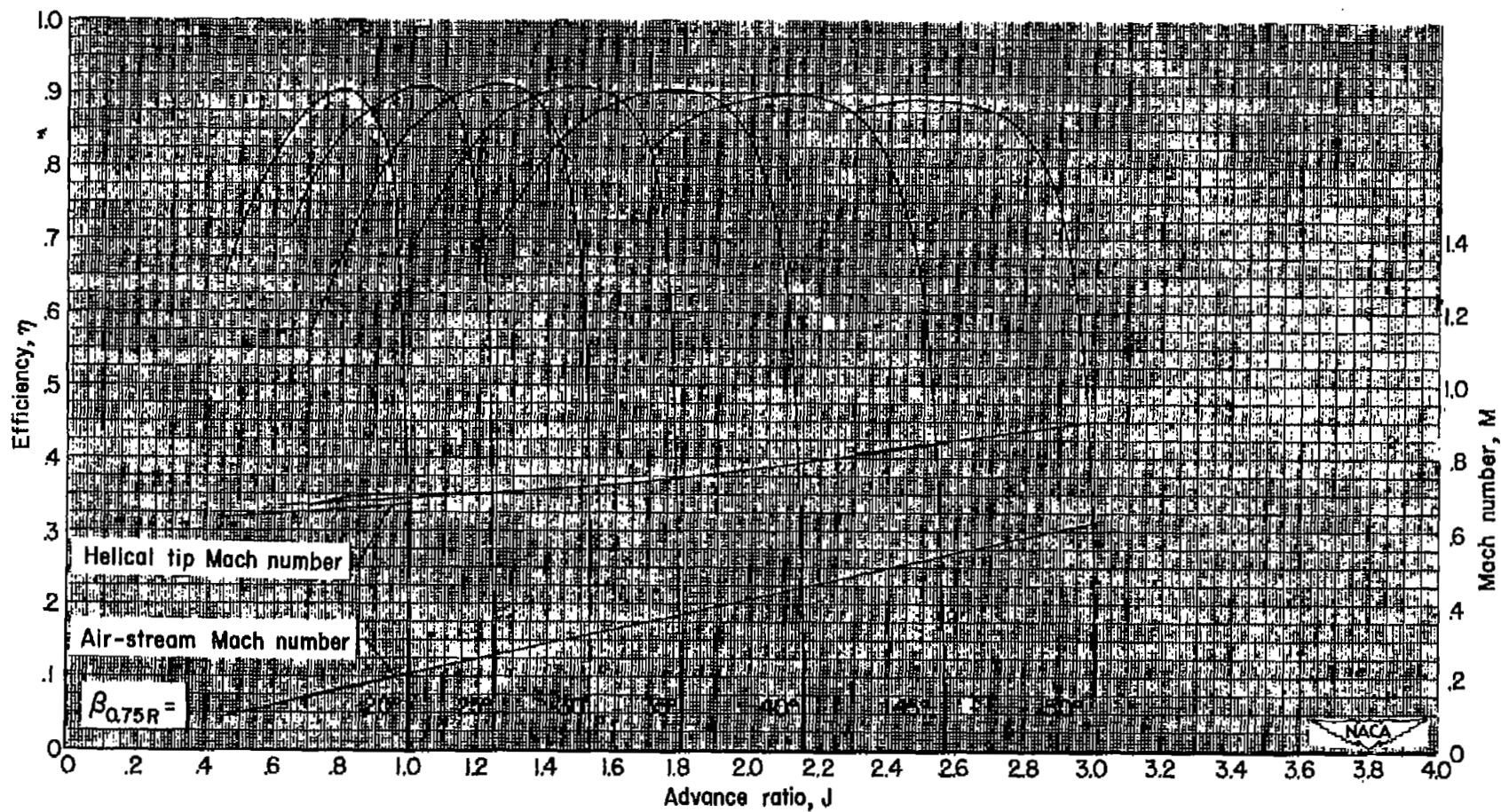
(a) Thrust coefficient.

Figure 4.- Characteristics of NACA 10-(3)(8)-03R propeller at 1350 revolutions per minute.



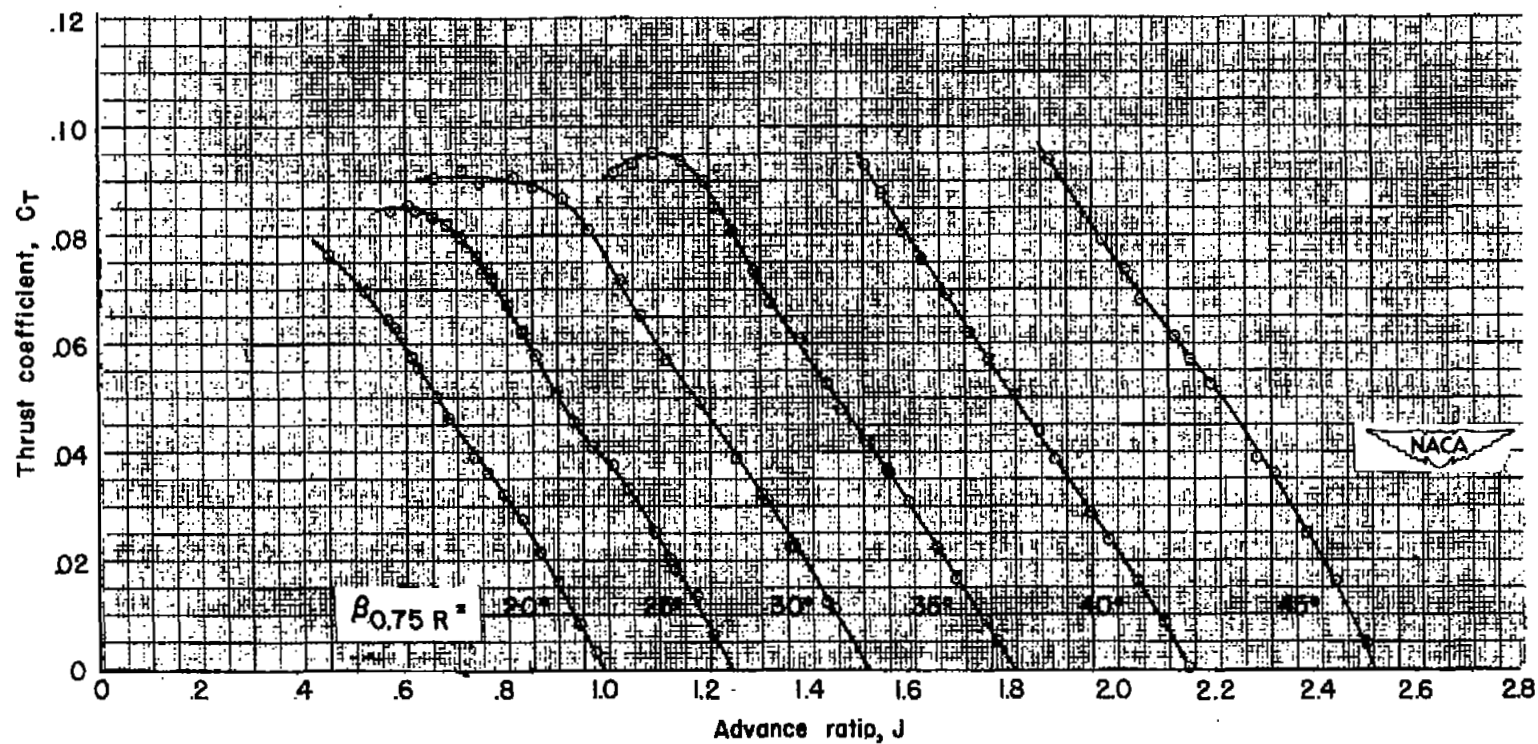
(b) Power coefficient.

Figure 4.- Continued. 1350 revolutions per minute.



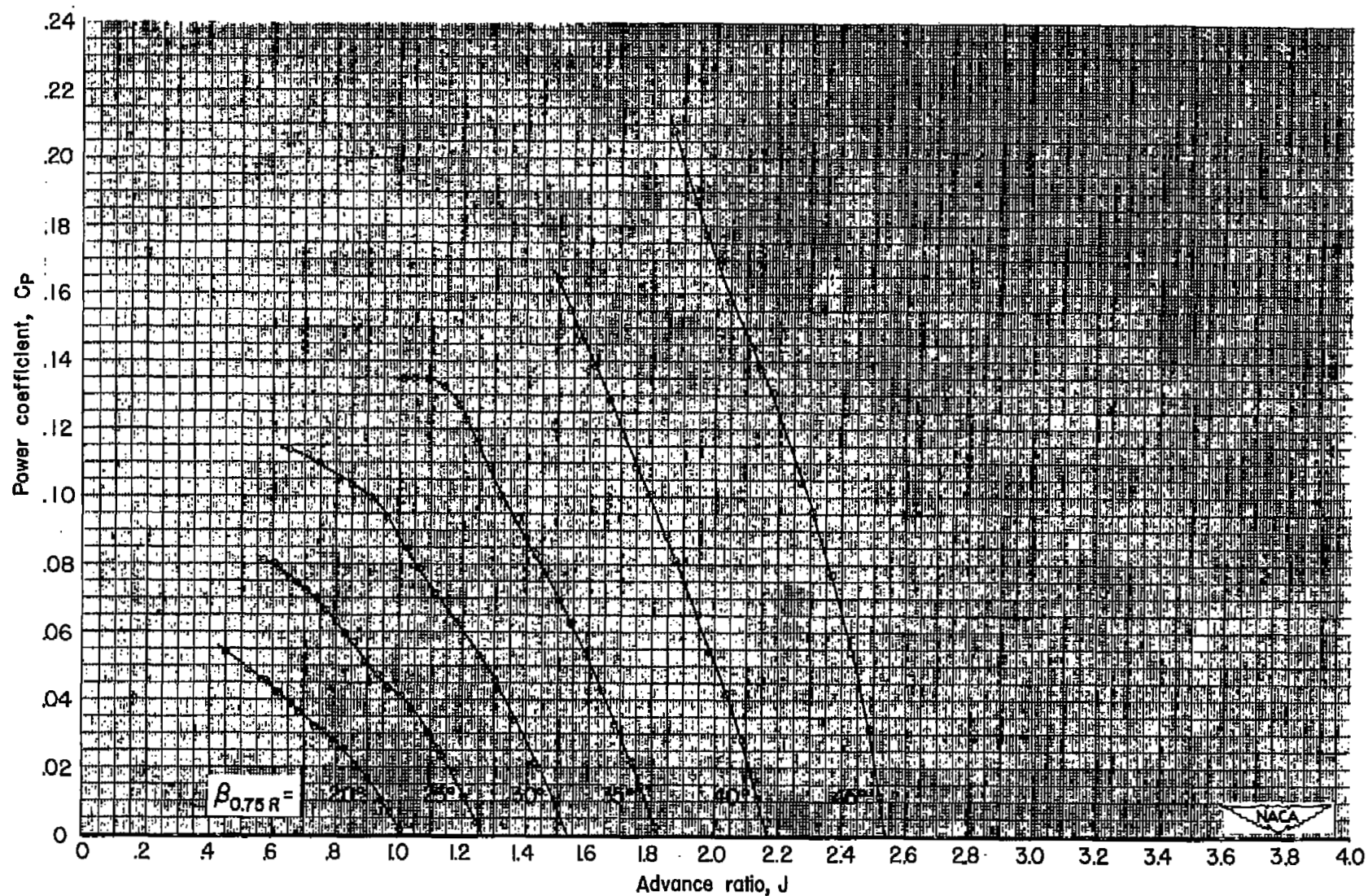
(c) Efficiency.

Figure 4.- Concluded. 1350 revolutions per minute.



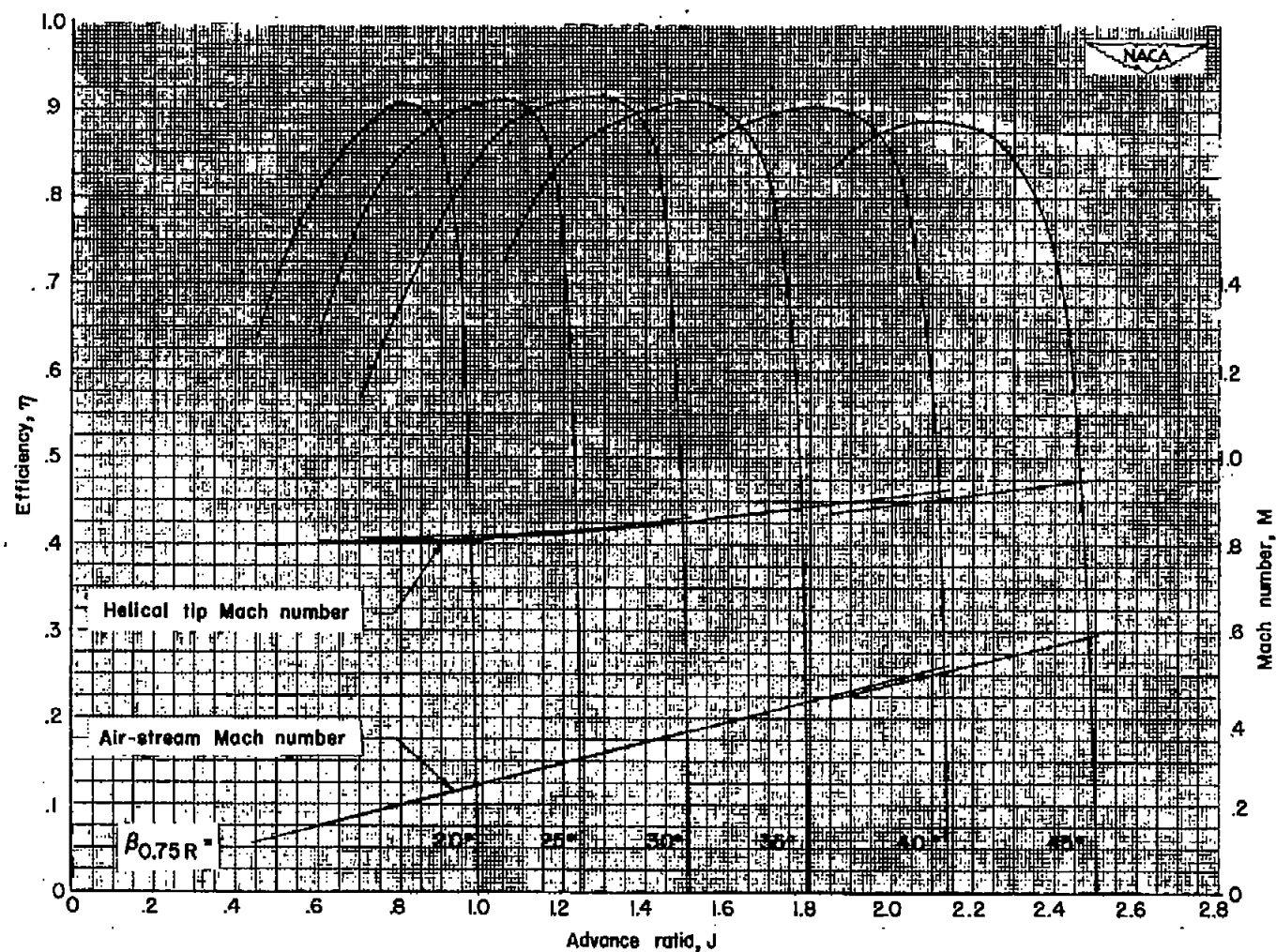
(a) Thrust coefficient.

Figure 5.- Characteristics of NACA 10-(3)(08)-03R propeller at 1600 revolutions per minute.



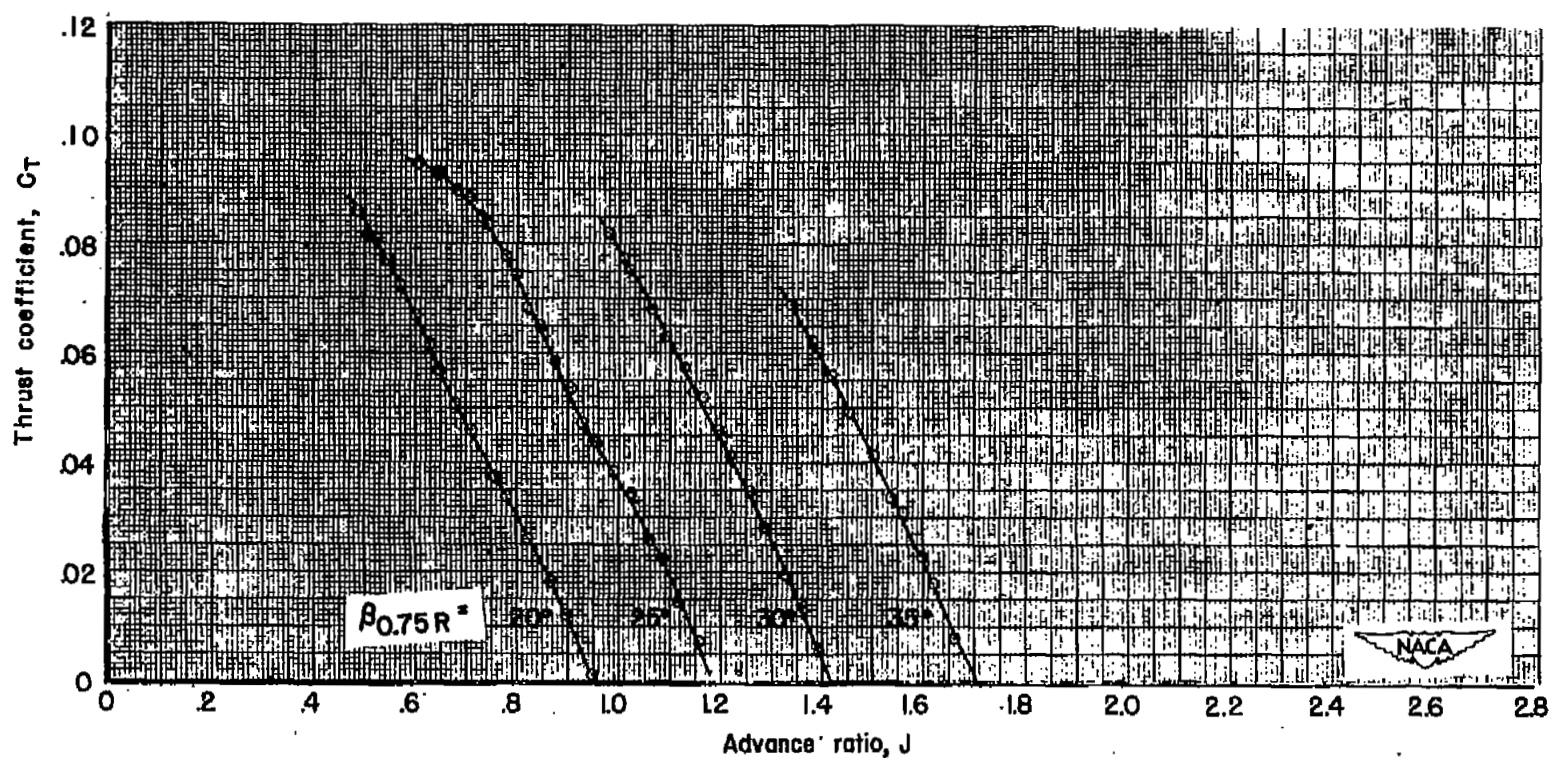
(b) Power coefficient.

Figure 5.- Continued. 1800 revolutions per minute.



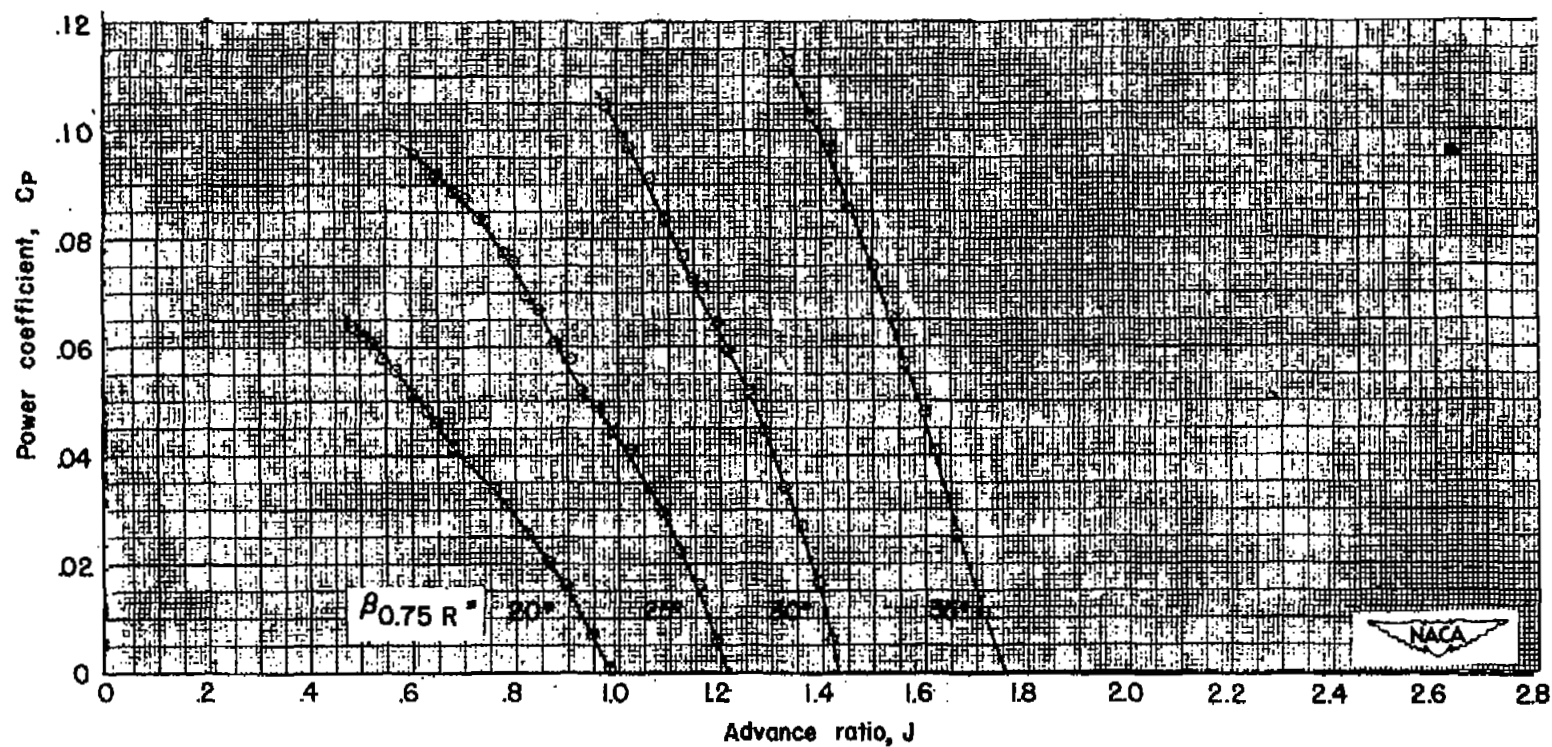
(c) Efficiency.

Figure 5.- Concluded. 1800 revolutions per minute.



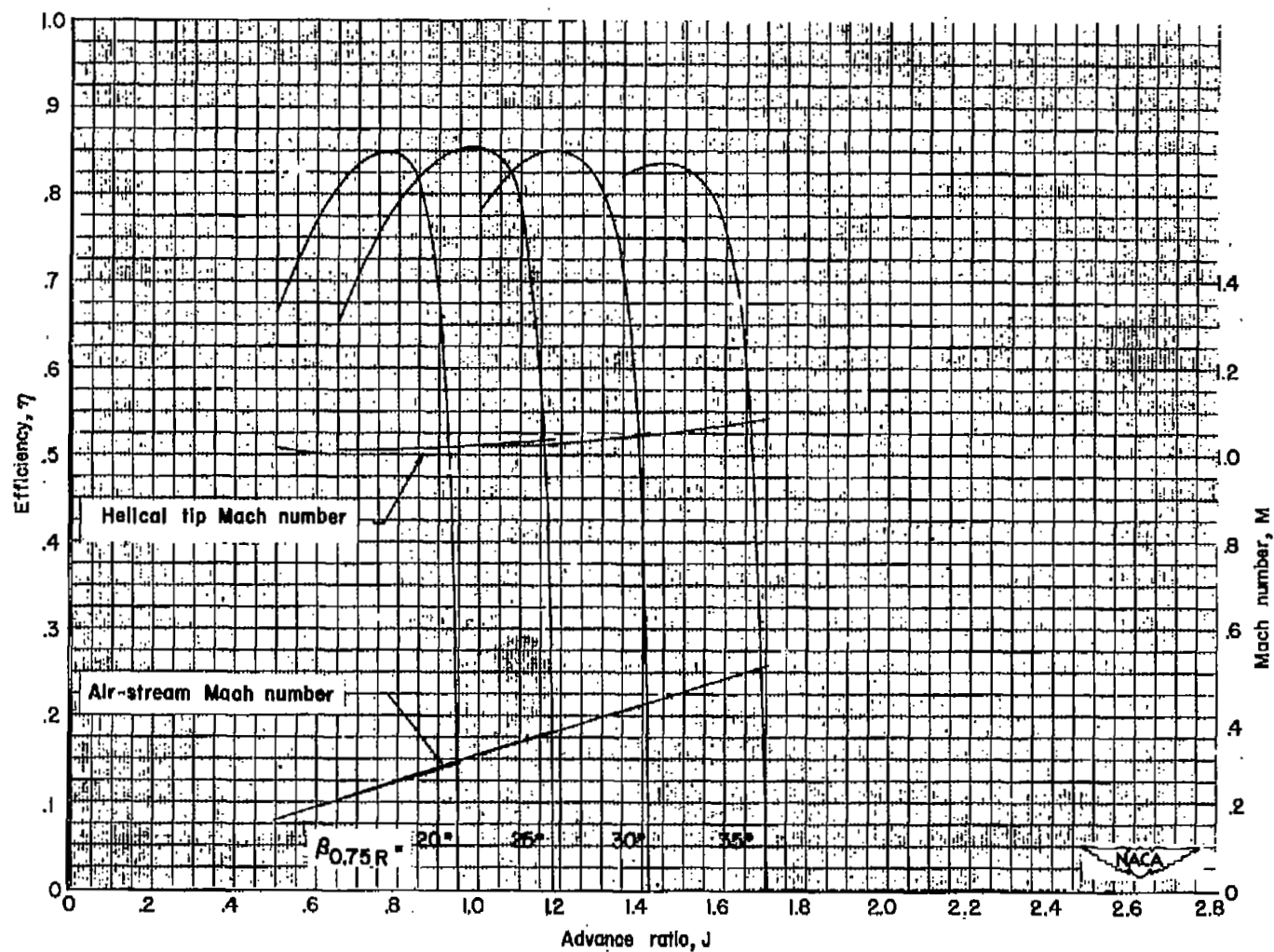
(a) Thrust coefficient.

Figure 6.- Characteristics of NACA 10-(3)(08)-03R propeller at 2000 revolutions per minute.



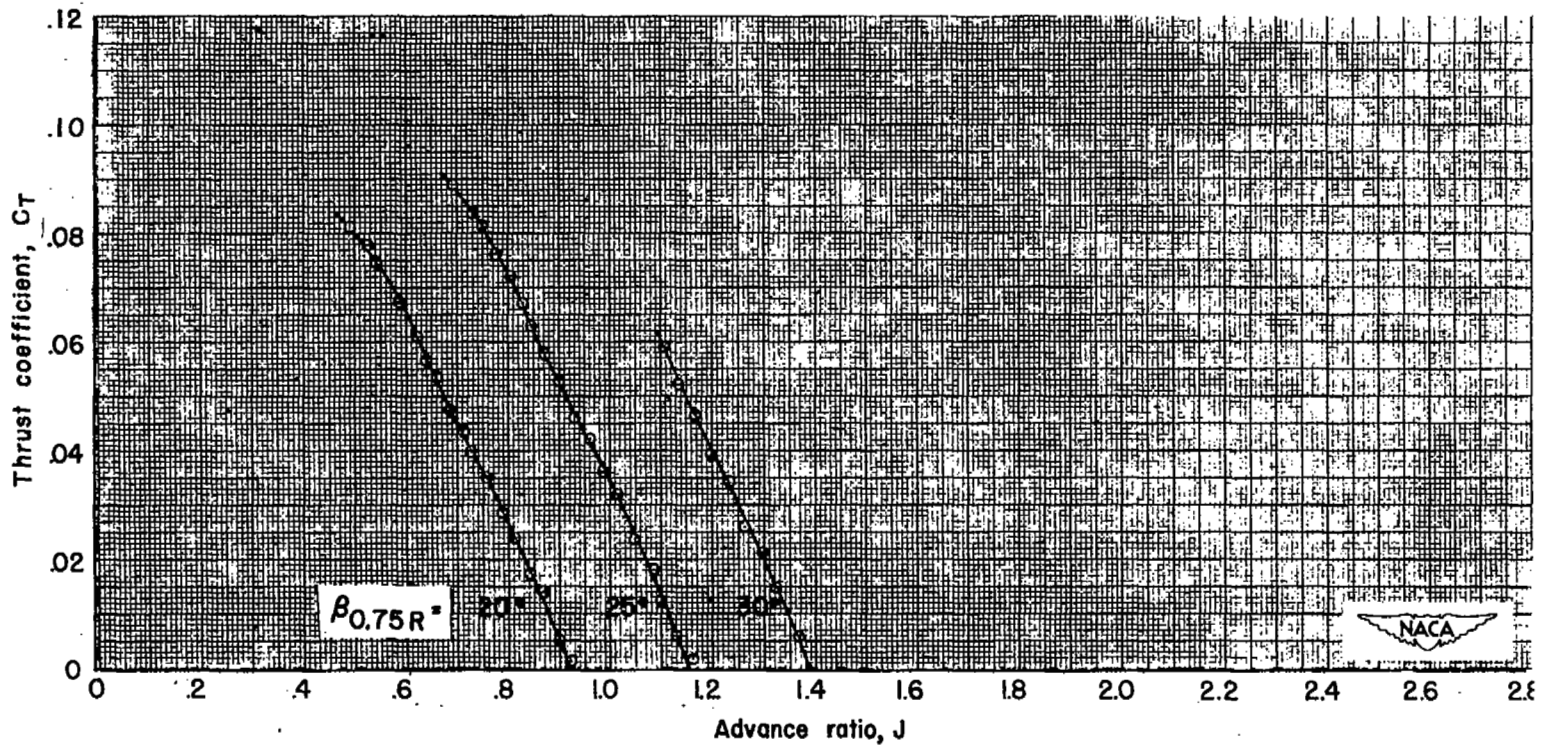
(b) Power coefficient.

Figure 6.- Continued. 2000 revolutions per minute.



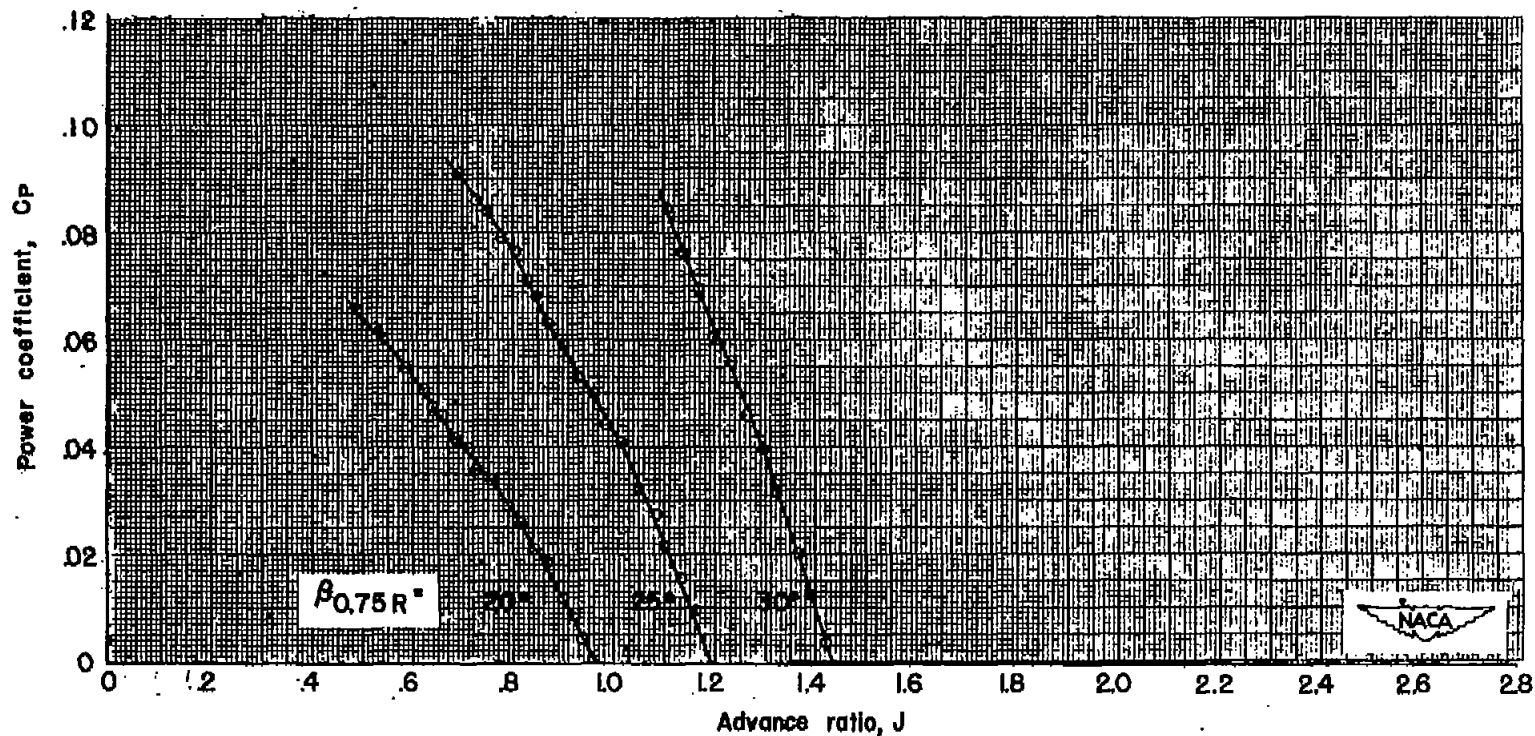
(c) Efficiency.

Figure 6.- Concluded. 2000 revolutions per minute.



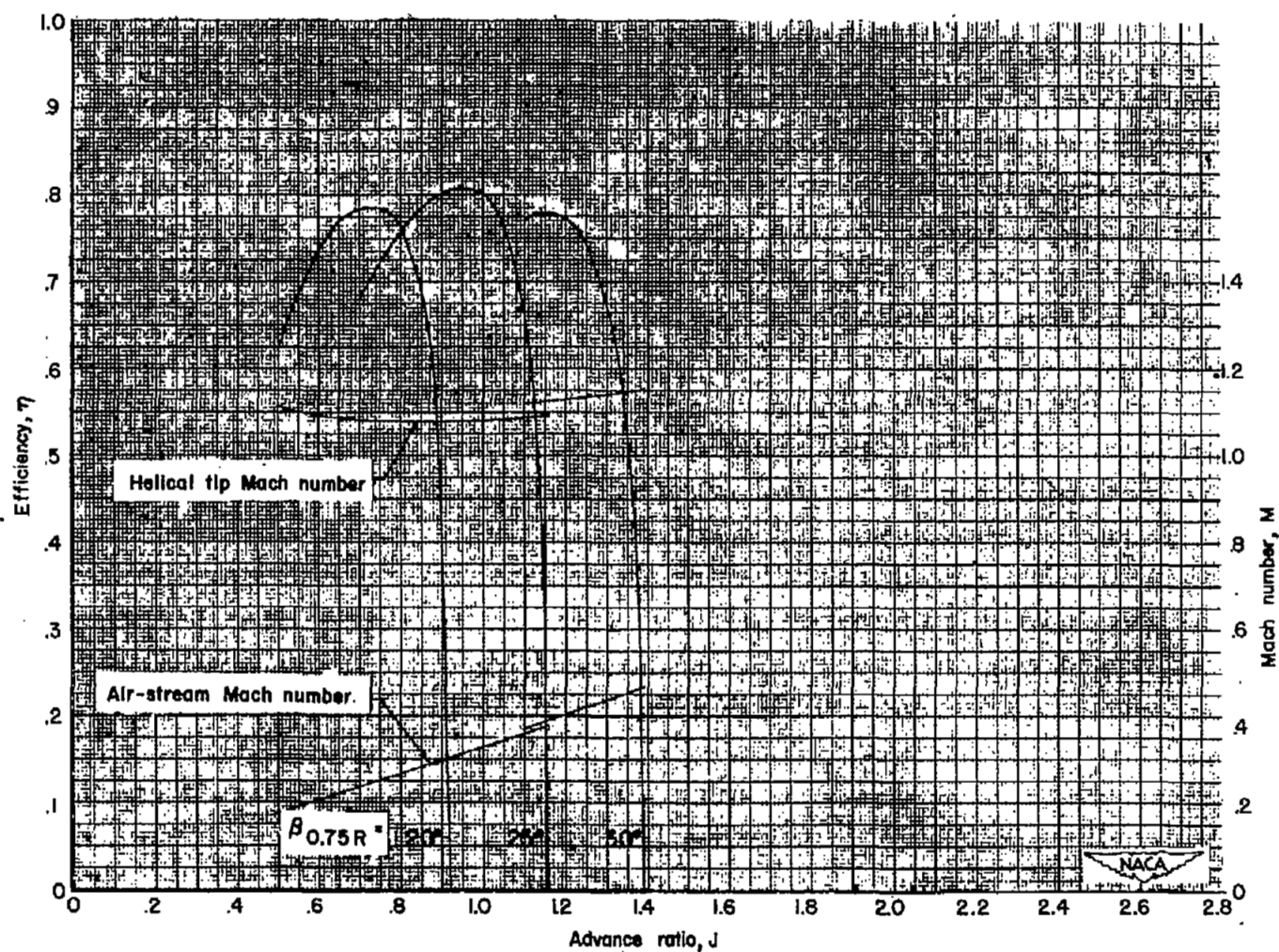
(a) Thrust coefficient.

Figure 7.- Characteristics of NACA 10-(3)(08)-03R propeller at 2160 revolutions per minute.



(b) Power coefficient.

Figure 7.- Continued. 2160 revolutions per minute.



(c) Efficiency.

Figure 7.- Concluded. 2160 revolutions per minute.

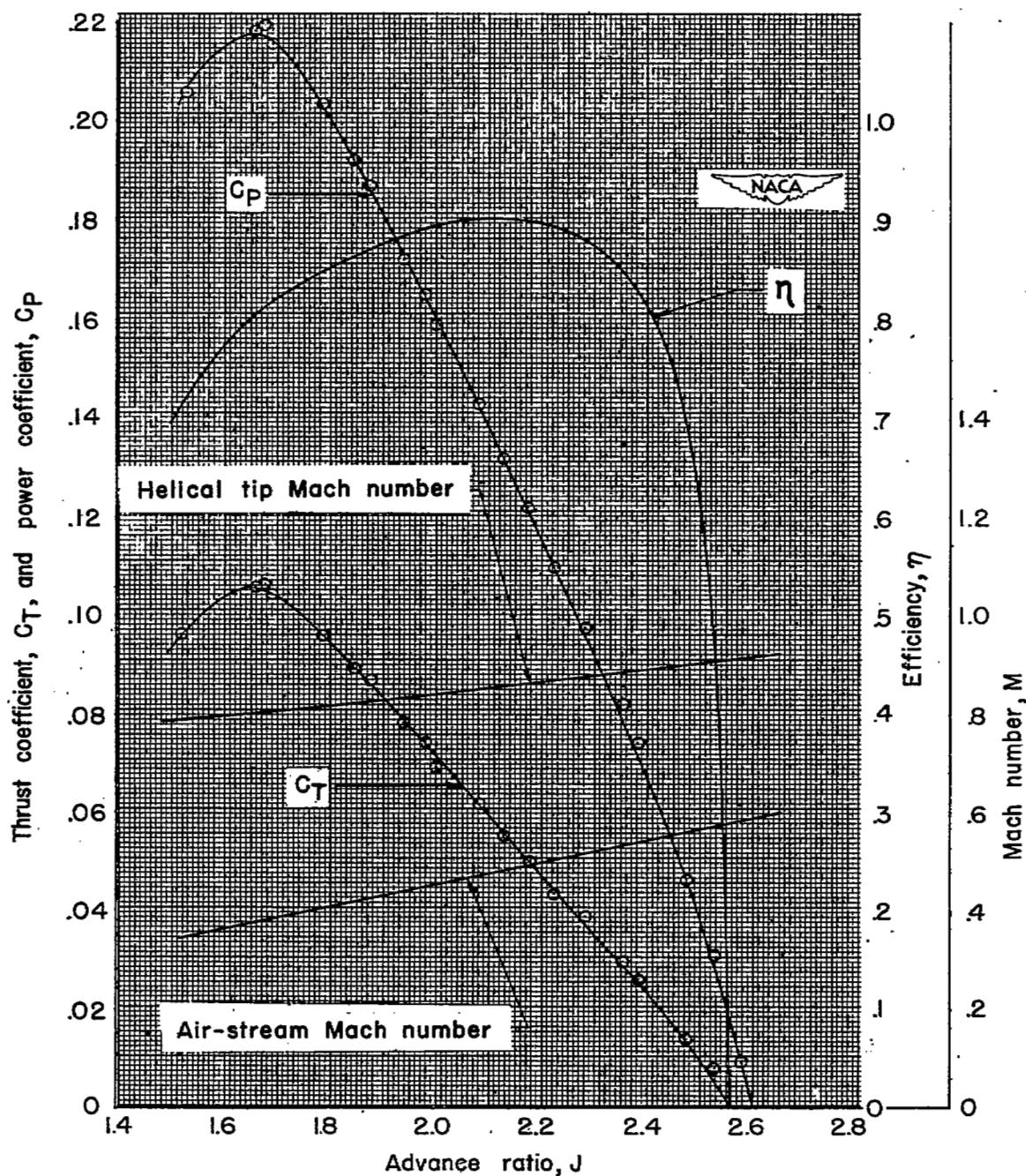
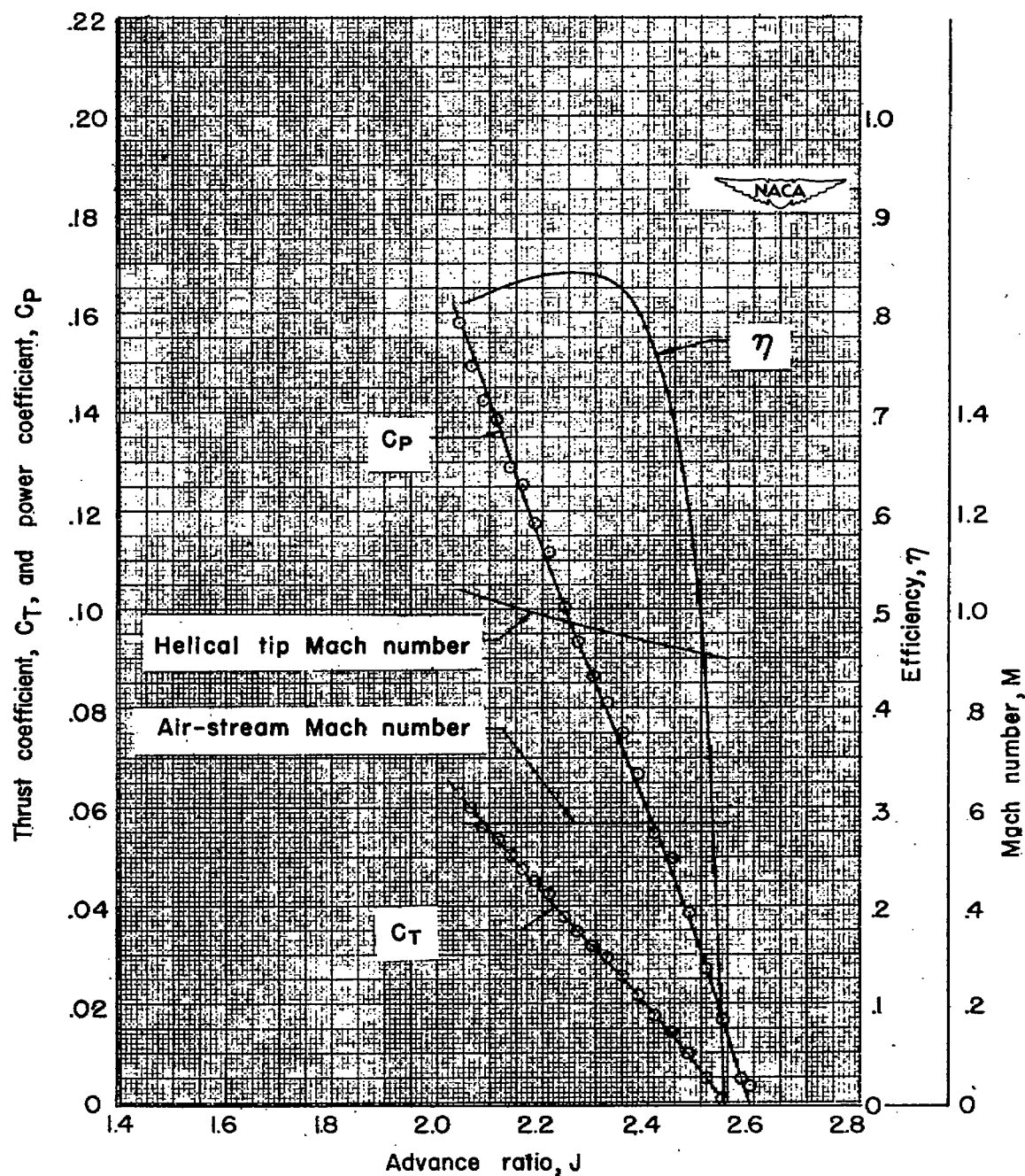
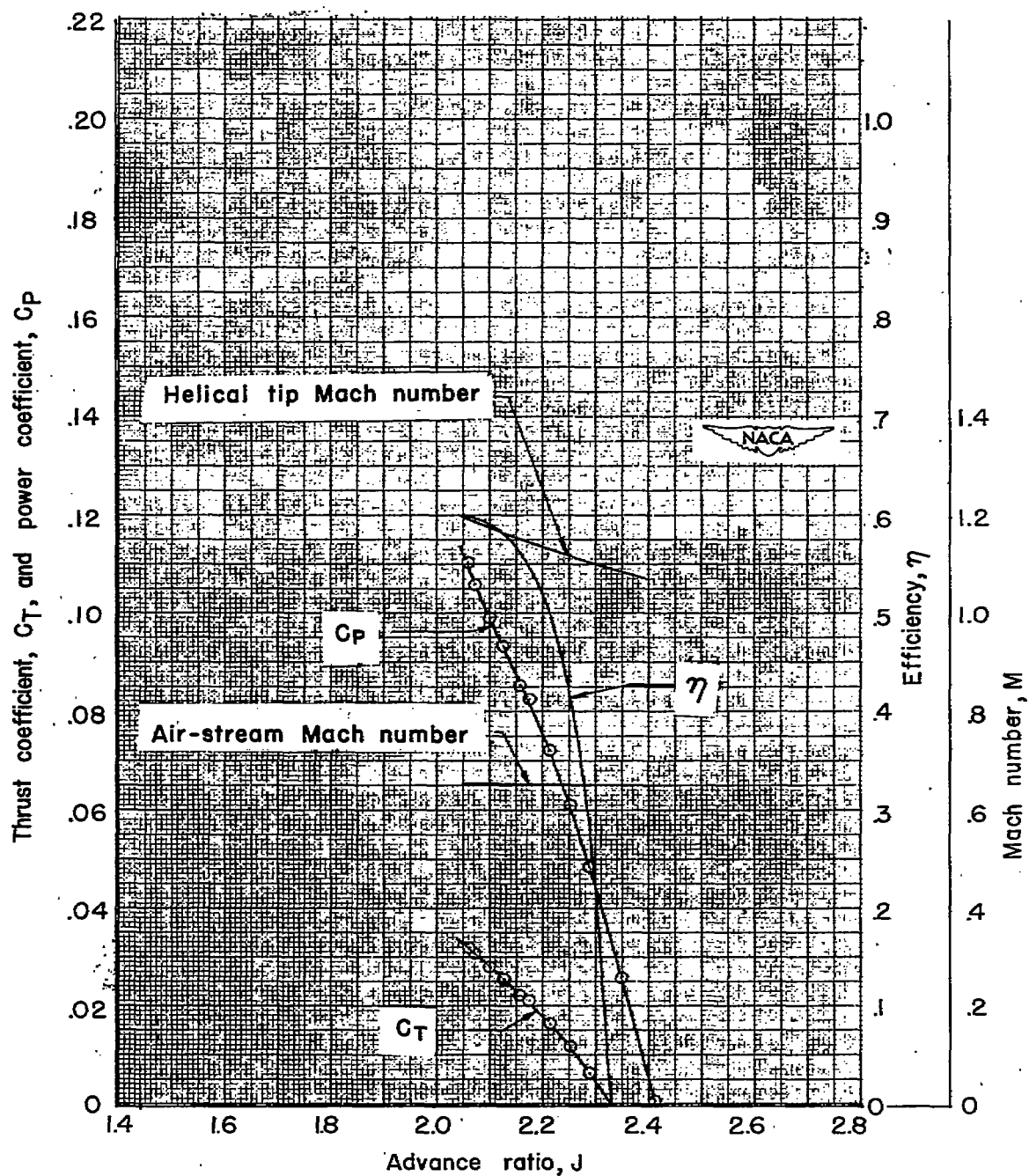


Figure 8.- Characteristics of NACA 10-(3)(08)-03R propeller at 1500 revolutions per minute. $\beta_{0.75R} = 45^\circ$.



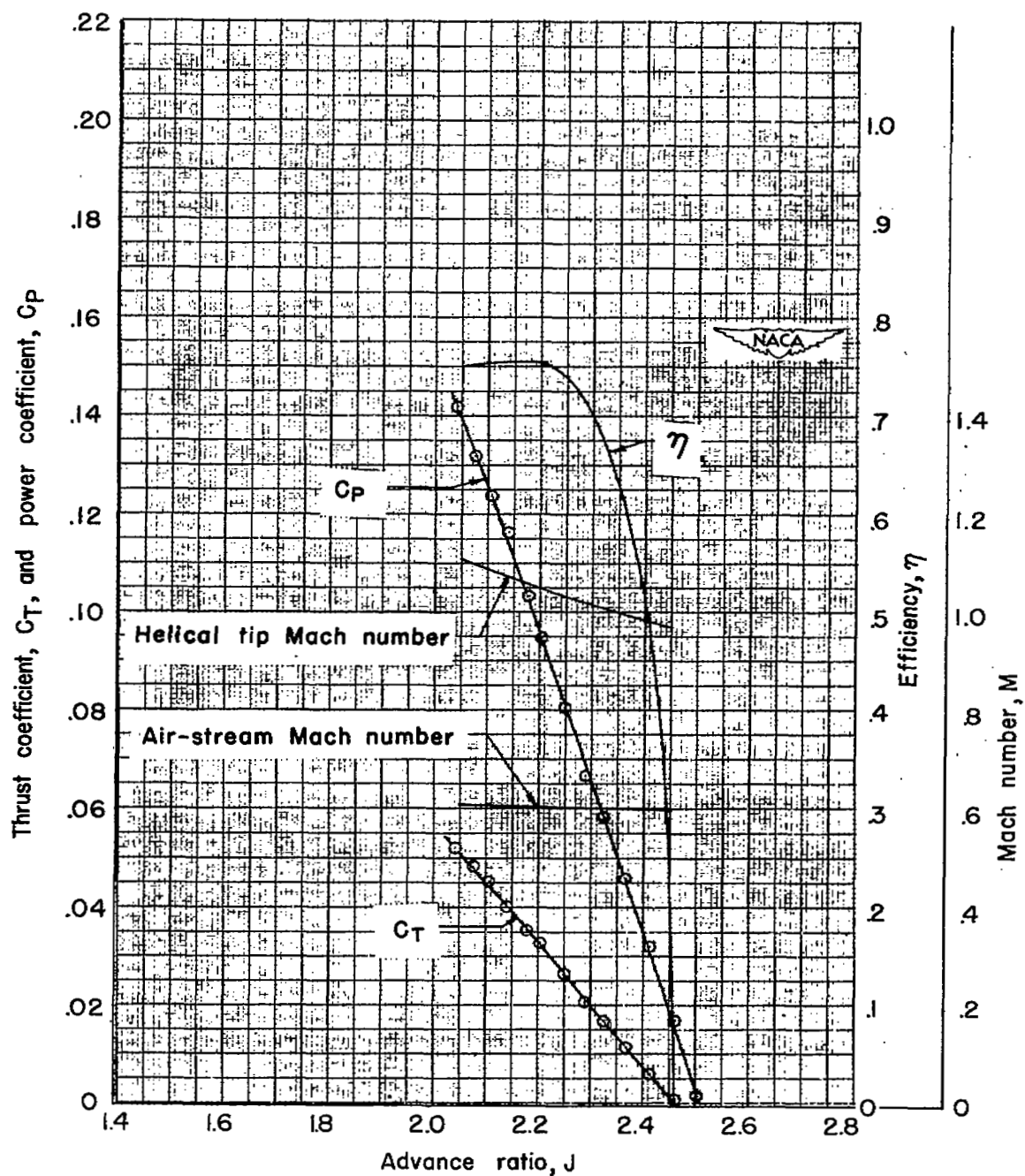
(a) Air-stream Mach number, 0.56.

Figure 9.- Characteristics of NACA 10-(3)(08)-03R propeller at high forward speeds. $\beta_{0.75R} = 45^\circ$.



(c) Air-stream Mach number, 0.65.

Figure 9.- Concluded.



(b) Air-stream Mach number, 0.60.

Figure 9.- Continued.

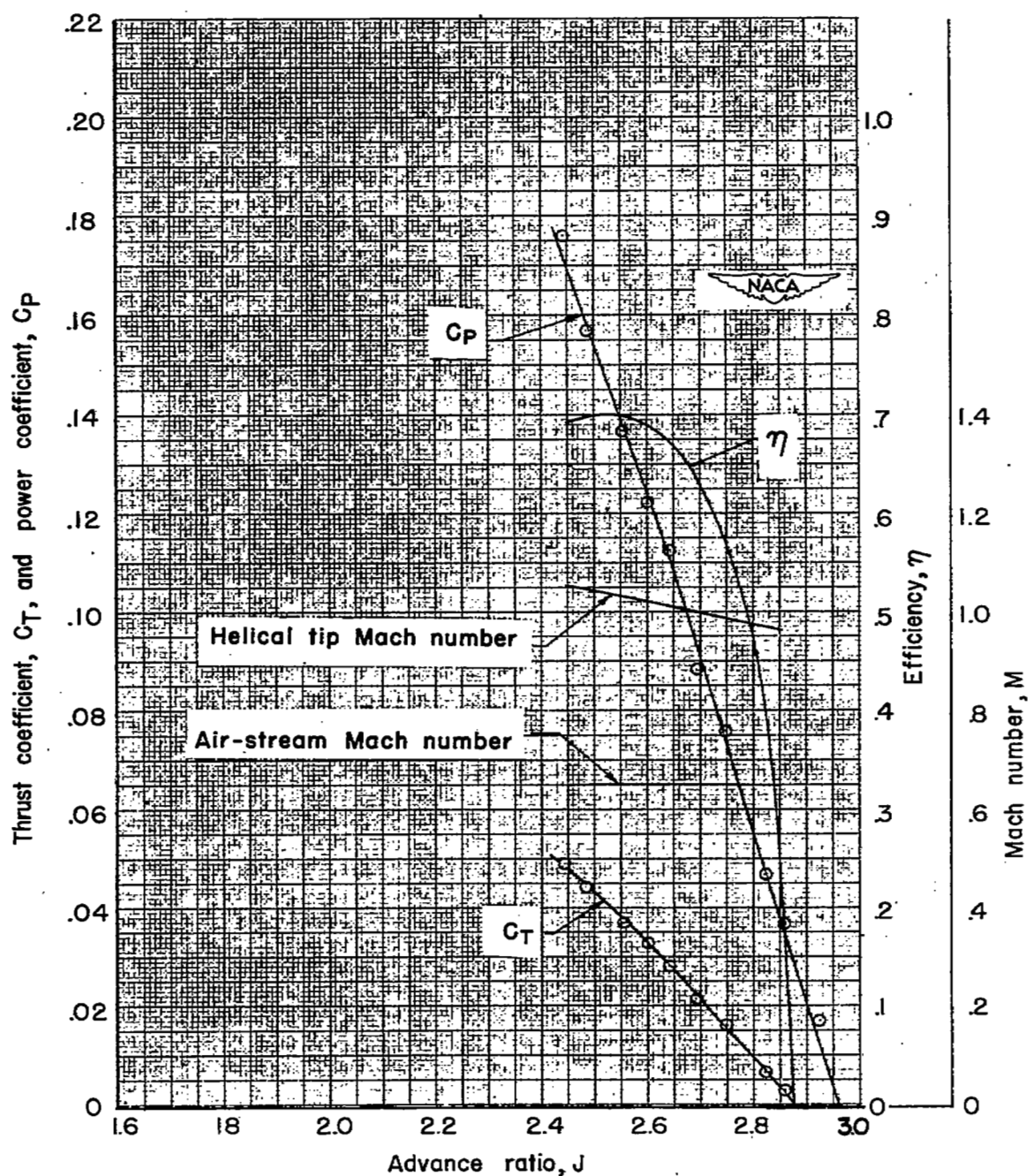


Figure 10.- Characteristics of NACA 10-(3)(08)-03R propeller.
 $\beta_{0.75R} = 50^\circ$; air-stream Mach number, 0.65.

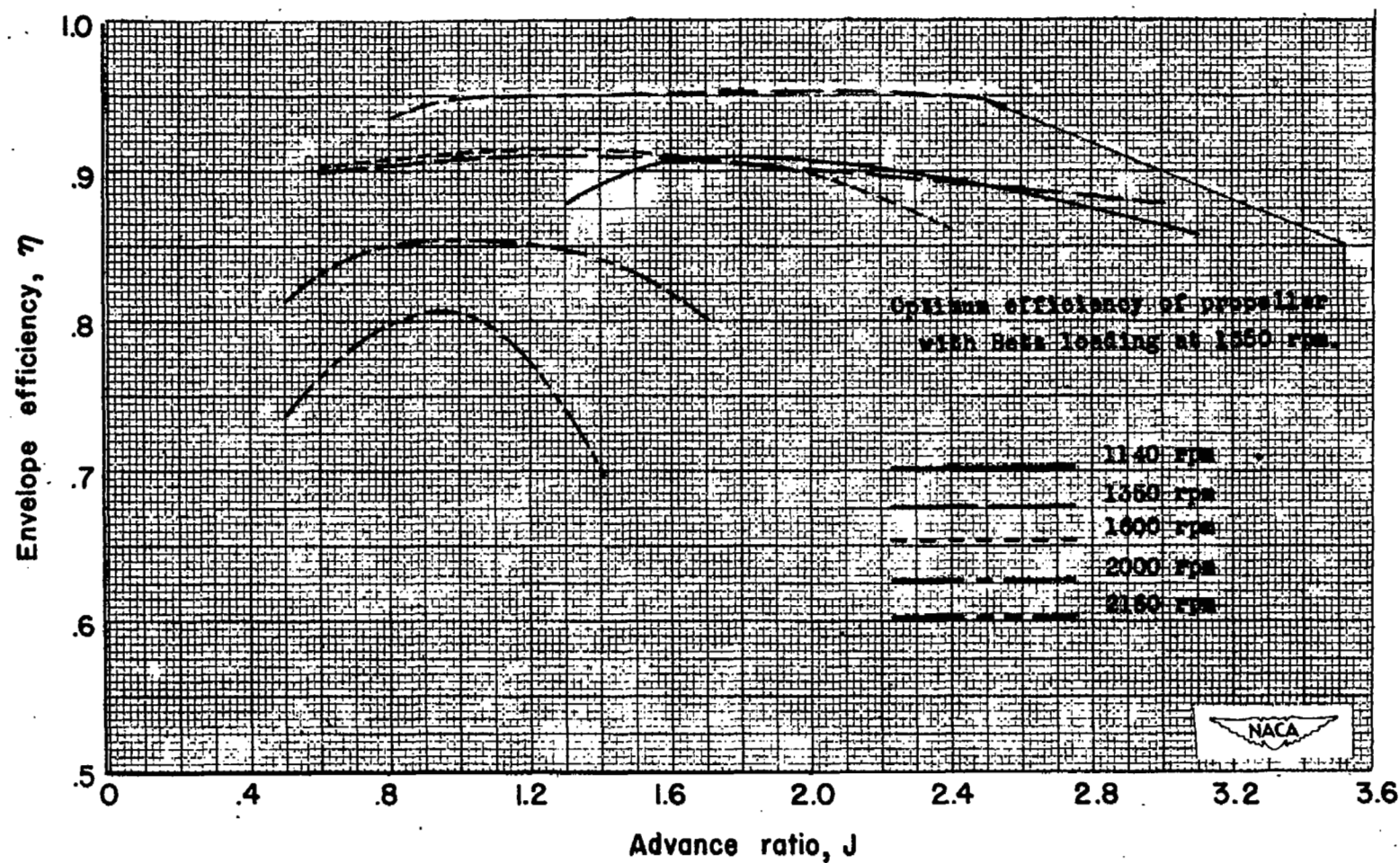


Figure 11.- Envelope efficiency of NACA 10-(3)(08)-03R propeller.

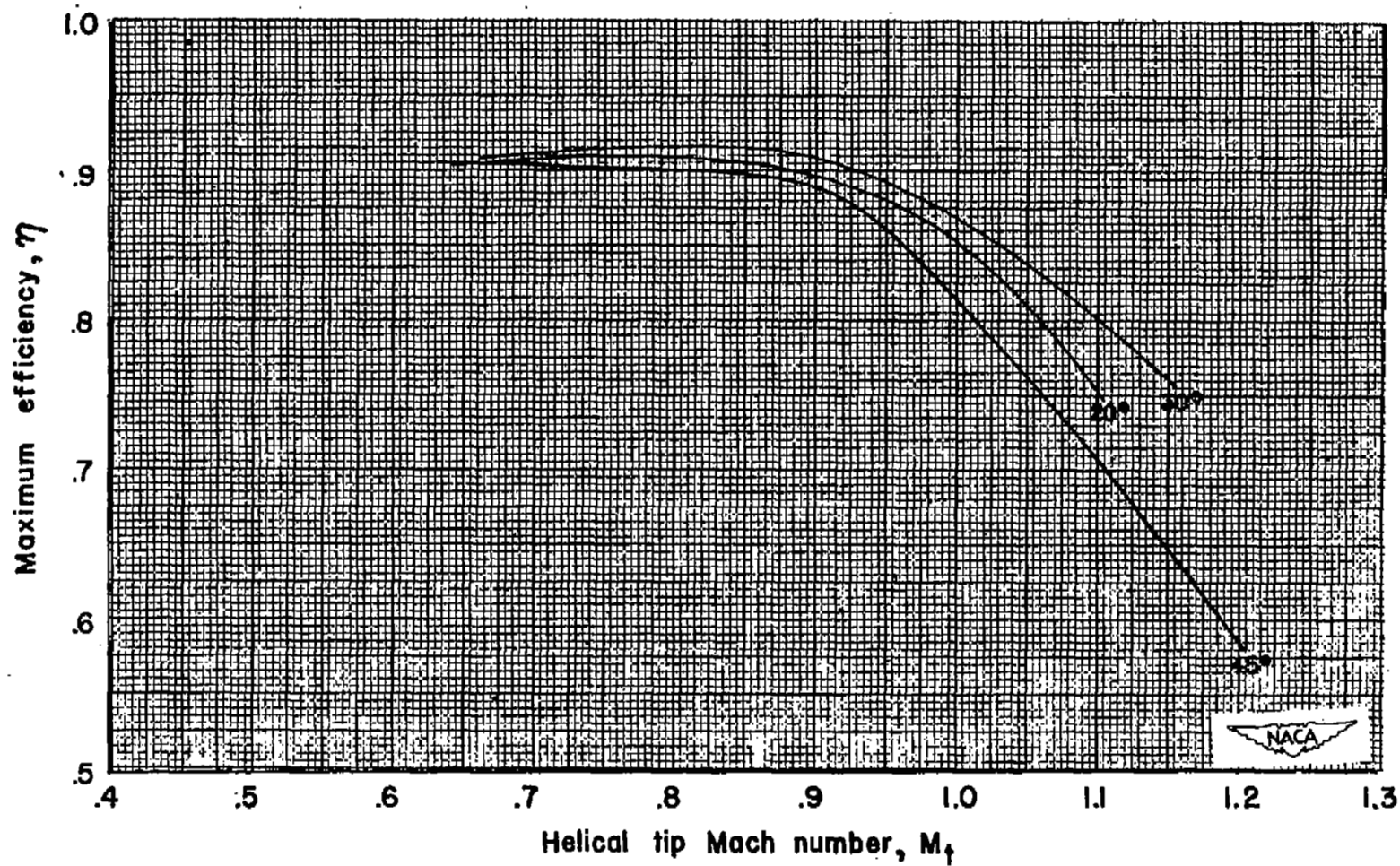


Figure 12.- Effect of helical-tip Mach number on maximum efficiency.

NASA Technical Library



3 1176 01436 6604